

Mechanisms of Primary Long-Lived Defect Production in Pure Quartz Glasses under Electron Irradiation

A. P. Sergeev and P. B. Sergeev

*Lebedev Physical Institute, Russian Academy of Sciences,
Leninskii pr. 53, Moscow, 119991 Russia; e-mail: psergeev@sci.lebedev.ru*

Received June 26, 2014

Abstract—Based on an analysis of the dependences of individual absorption band amplitudes in quartz glasses on the electron beam (EB) fluence, mechanisms of primary defect production in KS-4V, KU-1, and Corning 7980 glasses during their prolonged irradiation by EB pulses are determined.

DOI: 10.3103/S1068335614100029

Keywords: quartz glasses, KS-4V, KU-1, electron beam, absorption spectra, individual bands, long-lived defects.

In electron-beam excimer lasers (EBELs), output windows are exposed to X-rays and fast electrons scattered from the pump beam [1–4]. Upon exposure to these ionizing radiations, absorption increases in a material of laser windows, which can limit their functionality [5, 6]. Quartz glasses intended for operation with UV radiation are basic materials for large windows of high-power technological EBELs. This does dictate the necessity and direction of the experimental study of changes in the absorbance of KS-4V, KU-1, and Corning 7980 quartz glasses during long-term exposure to electron beam (EB) pulses and UV laser pulses [7–10].

The use of the method of decomposing complex spectra into individual bands (IBs) [11] in the analysis of experimental [7–10] spectra of the induced optical density of quartz glasses allowed the conclusion that these spectra in the range of ~ 160 – 350 nm consist of six IBs [10]. In [12, 13], the dependences of the amplitudes of these six bands (A_i) on the total EB energy density for a pulse train (hereafter, the EB fluence F) were obtained. The subscript i of A_i indicates the number of IB in Table 1 of [10], where the band parameters are given and the bands are referenced to absorption centers. It follows from Table 1 of [10] that the band with subscript 1 and an absorption maximum at 260 nm belongs to non-bridging oxygen atoms (NOA). The band with subscript 4 and a maximum at 213 nm belongs to E' -centers. The sixth band with a maximum at 163.5 nm is attributed to oxygen-deficient centers (ODCs). This indexation will be used in the present paper.

As for the defect types given in Table 1 in [10], we note the following. The induced EB absorption spectra were measured mostly in a day after irradiation. Hence, the corresponding IBs and their characteristics belong to arrays of long-lived defects of quartz glasses, formed by this time. The following lifetimes (τ_i) of these defect groups at storage temperatures of ~ 0 °C and in the absence of light reach 10^8 s and longer [8].

The determination of possible mechanisms of production of exactly such primary defect arrays (NOA, E' -centers, ODC) in quartz glasses during their irradiation with EB pulses with electron energies to 300 keV was the objective of the present study. To this end, the experimental dependences $A_i(F)$ obtained for KS-4V, KU-1, and Corning 7980 ArF Grade (hereafter, C-ArF) glasses are used [12, 13].

The choice of this basic triplet of defects is caused by the fact that exactly they control induced UV absorption in the UV region in pure quartz glasses, their nature is clear, and their absorption cross sections σ_i are known [14–16]. The knowledge of σ_i allows the most important for quantitative estimations transition from A_i to the surface defect density N_i (the integral of the defect density over the sample thickness), based on the relation

$$N_i = A_i/\sigma_i. \quad (1)$$

Table 1. Key characteristics of the production of the primary defects of quartz glasses at electron beam irradiation

Glass type	Defect type	$N_{\text{im}} \cdot 10^{-16}$, cm ⁻²	$n_{\text{im}} \cdot 10^{-18}$, cm ⁻³	F_{im} , J/cm ²	D_{im} , MGy	$\varepsilon_i \cdot 10^{13}$, J
KS-4V	NOA ($i = 1$)	2	1	1500	34	0.8
KU-1	NOA ($i = 1$)	10	5	1000	23	0.1
C-ArF	NOA ($i = 1$)	6	3	1000	23	0.2
KS-4V	E' -center ($i = 4$)	1.2	0.6	1500	34	1.2
KU-1	E' -center ($i = 4$)	4	2	1500	34	0.4
C-ArF	E' -center ($i = 4$)	2	1	1000	23	0.5
KS-4V	ODC ($i = 6$)	3.3	1.6	4000	91	1.2
KU-1	ODC ($i = 6$)	3.3	1.6	4000	91	1.2
C-ArF	ODC ($i = 6$)	—	—	—	—	~1

It is possible to describe the dependences $A_i(F)$ similar for all glasses (and, hence, $N_i(F)$), which reach a steady-state level with increasing F , by the simplest function

$$N_i = N_{\text{im}}[1 - \exp(-F/F_{\text{im}})]. \quad (2)$$

It is the solution to the differential equation

$$dN_i/dF = (N_{\text{im}}/F_{\text{im}}) - N_i/F_{\text{im}}. \quad (2a)$$

Here N_{im} is the steady number of i -th defects and F_{im} is the characteristic of the rate of reaching a maximum level. These parameters allow us to calculate the third parameter ($N_{\text{im}}/F_{\text{im}}$) defining the rise rate of the number of defects at the beginning of irradiation, related to the energy of the formation of corresponding defects (ε_i) as

$$\varepsilon_i = (N_{\text{im}}/F_{\text{im}})^{-1}. \quad (3)$$

We note that Eqs. (2a) are in essence kinetic equations for N_i , since the quantity F is a linear function of the sample irradiation time t : $F = W_s \cdot t$. Here W_s is the average specific EB power equal to the product of the EB fluence per pulse (F_1) and the average pulse repetition rate f . Taking into account this relation between F and t , it is sufficient to multiply all terms of Eq. (2a) by W_s to obtain the kinetic equation for N_i ,

$$dN_i/dt = (N_{\text{im}}/\tau_{\text{im}}) - N_i/\tau_{\text{im}}. \quad (2b)$$

Here $\tau_{\text{im}} = F_{\text{im}}/W_s$. Based on the sample irradiation conditions described in detail in [7–10, 12, 13], the EB fluence of 1000 J/cm² is reached in $\sim 10^6$ s.

The knowledge of N_{im} and the assumption that the distribution of the defect density (n_i) over the sample thickness x repeats the absorbed dose distribution $D(x)$ which is close to rectangular [12] allows us to estimate the maximum concentration of corresponding defects (n_{im}) using the equation

$$N_{\text{im}} = n_{\text{im}}/L_0. \quad (4)$$

Here L_0 is an effective thickness of EB irradiation of glasses, determined assuming the uniform distribution of the absorbed dose over the sample thickness with density $\rho = 2.2$ g/cm³ with maximum surface dose $D(0)$ at the EB fluence F_1 per pulse,

$$L_0 = F_1/D(0)\rho. \quad (5)$$

At $F_1 \approx 2$ J/cm², $D(0) \approx 40$ kGy, and $L_0 \approx 0.02$ cm [12].

The approximation of the rectangular distribution of the absorbed dose at the depth L_0 makes it possible to replace the values of F_{im} by dose values D_{im} using the relation

$$D_{\text{im}} = F_{\text{im}}/(L_0 \cdot \rho). \quad (6)$$

The values of N_{im} , n_{im} , F_{im} , D_{im} , and ε_i found properly from the experimental dependences $A_i(F)$ [12, 13] taking into account Eqs. (1)–(6) for KS-4V, KU-1, and Corning 7980 ArF Grade (C-ArF) quartz glasses are listed in corresponding columns of Table 1. In calculating N_{im} , we used the following absorption cross sections: $\sigma_1 = 5.3 \cdot 10^{-18}$; $\sigma_4 = 2.5 \cdot 10^{-17}$; $\sigma_6 = 7.5 \cdot 10^{-17} \text{ cm}^2$. The possible error of these values can reach 30% [14–16].

The N_i reaching of the steady-state level with increasing F , and hence, with the irradiation time t , can result from various causes. Let us consider two typical cases associated with two fundamentally different defect production mechanisms.

The first mechanism implies that the increase in the number of defects in time is compensated by their relaxation. This case is described by the well-known kinetic equation for the defect density n

$$dn/dt = W - n/\tau. \quad (7)$$

Here τ is the defect lifetime and W is the defect production rate proportional to the irradiation power. If these values are constant, the defect density reaches in time a steady level ($n_m = (W \cdot \tau)$) by the law

$$n = (W \cdot \tau)[1 - \exp(-t/\tau)]. \quad (7a)$$

The second case implies that defects are formed from certain “precursors” whose concentration is limited and supposed to be equal to p . In this case, the equation for the defect density can be written as

$$dn/dt = A(p - n) - n/\tau. \quad (8)$$

Here A is the coefficient characterizing the rate of “precursor” transformation to defects. It is proportional to the irradiation power. After simplest transformation, Eq. (8) takes the form

$$dn/dt = Ap - n(A + 1/\tau). \quad (8a)$$

It is identical to Eq. (7), but with other coefficients. Its solution has the form

$$n = [(Ap)/(A + 1/\tau)] \cdot [1 - \exp(-t(A + 1/\tau))]. \quad (8b)$$

If $A \gg 1/\tau$, Eq. (8b) becomes simpler,

$$n = p[1 - \exp(-tA)]. \quad (8c)$$

A comparison of Eqs. (8b) and (7a) shows that reaching the steady-state level is described by the same function in both cases. In the second case, steady defect density approaches the “precursor” concentration and, what is important, weakly depends on the irradiation power. Furthermore, in the exponent of $1/\tau$, the “precursor” burnout rate A is added in the second case. Sometimes, as in the case (8c), this rate can completely define the time of reaching the steady-state level. Hence, when interpreting the data obtained from almost identical in shape dependences $N_i(F)$, it is important to clearly determine the defect production process type.

To this end, we pay attention to the following experimental result. Irradiation of KU-1 and KS-4V glass samples by EB pulses was performed simultaneously in three different modes. In the first mode, samples were covered with a titanium foil layer 14–28 μm thick, F_1 was $\sim 2 \text{ J/cm}^2$. In the second mode, the titanium foil thickness was varied within 50–100 μm , and F_1 was from 0.3 to 0.9 J/cm^2 . In the third mode, the foil thickness was $\sim 140 \mu\text{m}$, and F_1 was $\sim 0.1 \text{ J/cm}^2$ [7–8, 12, 13]. The average EB energy was also varied: $\sim 300 \text{ keV}$ for the first mode, $\sim 100 \text{ keV}$ for the second mode, and no higher than 50 keV for the third mode.

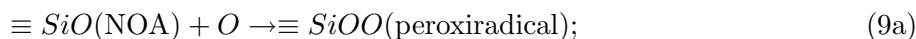
Experiments showed [7] that the steady optical density at 250 and 215 nm in KU-1 glass almost linearly increases with F_1 ; for KS-4V samples, it was almost identical during irradiation in the first and second modes. We do not consider the results on the third mode, since the steady level was not reached in this case. Since the EB pulse repetition rate f in these experiments was identical for all modes, the increase in F_1 reflects the increase in the average irradiation power. From this it follows that an increase in the number of NOAs and E' -centers in KU-1 can be described by Eq. (7), whereas the second case of the formation of these defects from “precursors” is implemented in KS-4V.

The experimental dependences $N_6(F)$ for KU-1 and KS-4V are almost identical and, what is important, this occurs under different irradiation conditions [12, 13]. This suggests the applicability of

the second approach to their interpretation. In this case, the ODC lifetime is much longer than that of NOAs and E' -centers, which validates the applicability of Eq. (8c).

The statement that primary defects in KS-4V glass are produced from “precursors” raises the question about their nature. “Stretched” bonds can play the role of such “precursors” during the formation of primary NOAs and E' -centers in this glass, and the production of ODCs is explained by hole localization on “compressed” bonds [13]. Hence, the values of n_{mi} of this glass, presented in Table 1, show the concentration level of corresponding “precursors”.

The formation of NOAs and E' -centers over the channel of “stretched” bond rupture in KS-4V should result in the same number of these defects, which is not consistent with Table 1 data. These differences can be associated with relaxation processes. We recall that sample irradiation with EB pulses lasted about one year [7, 8]. The excess of the number of NOAs over E' -centers can be explained by the interaction of primary defects with interstitial oxygen appearing during the ODC formation. Indeed, at identical rates of the interaction of oxygen in reactions



the number of E' -centers will decrease, while the number of NOAs will remain unchanged, since their decrease due to the former reaction is compensated by the inflow in the latter. The estimations of the numbers of NOAs and E' -centers ($F \approx 4 \text{ kJ/cm}^2$), performed taking into account the number of oxygen atoms thrown into interstices during the formation of ODCs by the time of reaching the steady-state level, show that this mechanism explains with good accuracy the observed inequality of the production of the primary defect pair. From this it also follows that exactly the number of NOAs in KS-4V in Table 1 column of n_{im} most accurately reflects the level of “stretched” bonds in this glass.

ODCs formed in KS-4V and KU-1 glasses under electron irradiation are very stable. After EB irradiation, their number in samples was almost unchanged within four storage years. Irradiation of the same samples by the ArF laser also did not change the number of ODCs [10]. Hence, the values of n_{6m} in Table 1 reflect the level of ODC “precursors” which can be “compressed” bonds [13].

The closeness of NOA and ODC formation energies in KS-4V indicate the closeness of concentration levels of their “precursors”, i.e., “stretched” and “compressed” bonds and similarity of their transformation stimulation mechanisms. In both cases, this is hole localization on them.

As seen in Table 1, the numbers of ODCs in KS-4V and KU-1 under saturation conditions are identical. Hence, the concentrations of their “precursors”, i.e., “compressed” bonds should also coincide. They, as is known, are defined by the glass-transition temperature [17]. This is also true for the “stretched” bonds, i.e., their number in KU-1 is the same as in KS-4V. Then, the NOA and E' -center production via “stretched” bond breaking in KU-1 generates the same number of these defects as in KS-4V. In the units of concentration, this is $\sim 10^{18} \text{ cm}^{-3}$, which is to 20% of the entire number of NOAs in KU-1 and to 50% of E' -centers.

We can see in Table 1 column of ε_i that the NOA formation energies in “wet” KU-1 and C-ArF glasses with a hydroxyl concentration of $\sim 1000 \text{ ppm}$ are close, but significantly lower than the similar energy of KS-4V which belongs to the group of “dry” glasses with hydroxyl contents less than 1 ppm. Hence, “wet” glasses have additional and efficient mechanisms of NOA production under electron irradiation.

First of all, this is H detachment from the $\equiv SiOH$ complex, which was discussed previously [10, 12, 13]. The concentration of such complexes in “wet” glasses under study is $\sim 10^{20} \text{ cm}^{-3}$. However, the formation of long-lived $\equiv SiO$ complexes, i.e., NOAs, is first of all possible in the absence of a reverse process. The latter is removed by bonding free hydrogen atoms at interstitial oxygen or chlorine. Therefore, the concentration of these gases in the interstice will define the number of NOAs formed in this process [10]. If each oxygen atom in the interstice binds two hydrogen atoms, and the number of oxygen atoms is the same as the number of ODCs in KS-4V, $\sim 3 \cdot 10^{18} \text{ cm}^{-3}$ or $\sim 60\%$ of the total number of NOAs are formed in KU-1 due to this process.

Hydrogen atom detachment from the $\equiv SiOH$ complex can cause production of the primary defect pair in the presence of the reverse process as well. Thus, if the detached H atom will not return to its

site, but will bind with a NOA of a short-lived complementary pair formed by breaking a regular $\equiv\text{Si}-\text{O}-\text{Si}\equiv$ bond, primary NOAs and E' -centers will be spatially separated, which transfer them to the class of long-lived ones [10]. Estimations show that up to $\sim 10^{18} \text{ cm}^{-3}$ of NOAs and E' -centers are produced via this third channel in KU-1, which is ~ 20 and $\sim 50\%$ of their total content.

According to specifications, the chlorine content in Corning 7980 Base Grade, KrF Grade, and ArF Grade glasses is ~ 100 , 50, and 20 ppm, respectively, at the same hydroxyl content of 800–1000 ppm. The induced optical density in the UV region of this glass group under saturation conditions differed only by 10% [8]. This suggests that the observed differences in the absorbance of KU-1 and C-ArF glasses are caused not so much by the differences in the Cl content, but by the hydroxyl content. We recall that the hydroxyl content in KU-1 is from 1000 to 2000 ppm.

The results presented in F_{im} and D_{im} columns of Table 1 reflect the rate of reaching the steady-state level by the number of corresponding defects, which is achieved at approximately $3F_{\text{im}}$. In KS-4V glass, the production rate of NOAs and E' -centers is defined by the rate of “stretched” bond burnout; hence, it is identical for both defects. The dominance of different channels of production of these defects in “wet” glasses also controls the difference of their rate of reaching the steady-state level. The lower ODC formation rate in KS-4V and KU-1 in comparison with the NOA production rate can be explained by the almost three times lower quantum efficiency of the processes occurring during hole localization on “compressed” bonds.

Thus, the presented analysis of the dependences of the amplitudes of IBs belonging to primary defects of quartz glasses on the EB fluence revealed the differences in the defect formation processes in them. For high-purity KS-4V quartz glass, the basic mechanism of NOA and E' -center formation is breaking the “stretched” bonds during hole localization on them. A similar process on “compressed” bonds leads to ODC formation and oxygen atom ejection to interstices. Their interaction with NOAs and E' -centers results in a decrease in the concentration of these centers and the formation of new defects, in particular, peroxiradicals absorbing most likely in the band at 183 nm. In “wet” glasses with high hydroxyl contents (KU-1 and C-ArF), the processes occurring during breaking “strained” bonds described above are accompanied by NOA production processes when hydrogen is detached from the hydroxyl group and by the interaction of hydrogen atoms ejected into interstices with oxygen and short-lived NOAs. These processes lead to an increase in the yield of long-lived NOAs in studied glasses by a factor from 3 to 5 and an increase in the yield of E' -centers by a factor to 2.

The results obtained show that, among the studied quartz glasses, the least level of EB-induced steady absorption in individual bands belonging to NOAs and E' -centers is inherent to high-purity “dry” KS-4V glass. The determination of the radiation defect formation mechanisms in this glass points to possible ways to further increase its radiation strength, i.e., the methods for decreasing the number of “strained” bonds should be sought. In particular, this can be their annealing by VUV light or X-rays in the presence of hydrogen, water, methane, or other gases in glass interstices to transfer NOAs and E' -centers formed during irradiation to $\equiv\text{SiOH}$ complexes.

REFERENCES

1. V. S. Barabanov, N. V. Morozov, and P. B. Sergeev, *Kvant. Elektron.* **18**, 1364 (1991).
2. V. S. Barabanov, N. V. Morozov, and P. B. Sergeev, *J. Soviet Laser Res.* **14**, 286 (1993).
3. A. V. Amosov, V. S. Barabanov, S. Yu. Gerasimov, et al., *Kvant. Elektron.* **20**, 1077 (1993).
4. V. S. Barabanov and P. B. Sergeev, *Kvant. Elektron.* **22**, 745 (1995).
5. V. G. Bakaev, E. V. Polyakov, G. V. Sychugov, et al., *Proc. SPIE* **5137**, 323 (2003).
6. I. A. Mironov, V. M. Reiterov, A. P. Sergeev, et al., *Proc. SPIE* **5479**, 135 (2004).
7. P. B. Sergeev, T. A. Ermolenko, I. K. Evlampiev, et al., *Opt. Zh.* **71**(6), 93 (2004).
8. P. B. Sergeev, A. P. Sergeev, and V. D. Zvorykin, *Kvant. Elektron.* **37**, 706 (2007).
9. P. B. Sergeev, A. P. Sergeev, and V. D. Zvorykin, *Kvant. Elektron.* **37**, 711 (2007).
10. P. B. Sergeev and A. P. Sergeev, *Kvant. Elektron.* **40**, 804 (2010).
11. M. V. Fok, *Trudy FIAN* **59**, 3 (1972).
12. A. P. Sergeev and P. B. Sergeev, *Opt. Zh.* **78**(5), 77 (2011).
13. A. P. Sergeev and P. B. Sergeev, *Kratkie Soobshcheniya po Fizike FIAN* **38**(12), 21 (2011) [*Bulletin of the Lebedev Physics Institute* **38**, 360 (2011)].
14. K. Saito, A. J. Ikushima, T. Kotani, and T. Miura, *J. Appl. Phys.* **86**, 3497 (1999).
15. L. Skuja, H. Hosono, and M. Hirano, *Proc. SPIE* **4347**, 155 (2001).
16. K. Kajihara, M. Hirano, L. Skuja, and H. Hosono, *Phys. Rev. B* **78**, 094201 (2008).
17. K. Awazu and H. Kawazoe, *J. Appl. Phys.* **94**, 6243 (2003).